Turkish Online Journal of Qualitative Inquiry (TOJQI)
Volume 12, Issue 3, June 2021: 4580 - 4593

Research Article

INVESTIGATION ON INERTIA FRICTION WELDING ANALYSIS PROCESS ON TI-CU MATERIAL THROUGH LINEAR CONDITION

B. Ramesh [a*], S. Satish Kumar [b]

Absract

Friction welding's basic principle was intermetallic bonding at the point of superplasticity achieved with self-generating heat due to finished upset strain and friction. Different metal connections are now particularly common in the fields of defense, aerospace, automotive, biomedical, refining, and nuclear engineering. Because of their low bonding strength, some special alloys with dual phases cannot be successfully joined by friction welding. The metallurgical transformations in an interfacing line on the alloy surfaces after bonding are also visible. Research is scarce in this field that has been published. Although several trials were conducted to obtain a Region of sound weld in an uninterrupted connection between Tie6Ale4V and SS304L, the joint is not effective. The friction welding properties of Tie6Ale4V and SS304L with pure OFC as an overlay were analyzed in this paper. To reduce the number of experiments required, the BoxeBehnken design was used. The automatic strength of the weld joint was investigated. The highest tensile strength was obtained between Tie6Ale4V and SS304L, where pure Cr was used as the insert metal. EDS was used to perform structural and microstructural investigations. XRD analysis was used to identify the formation of a metal matrix at the interface.

Keywords: Friction welding, titanium, copper, mild steel, dissimilar, tensile test, xrd analysis

Introduction

Because of its superior erosion conflict and unique strength related to steel, titanium is ideal for the chemical and aerospace industries. Q302 [1] metal has high power and a lower price than titanium. One of the most commonly used methods for producing bimetallic sheets is volatile. During the welding process, the insert plate was chosen as CP-Ti, and the base plate was obtained as Q345 Explosion-bonded CP-Ti/ Q345 bimetallic sheets will completely leverage the two materials' corresponding benefits.

[a]Institute of Mechanical Engineering, Saveetha School of Engineering, Saveetha Institute of Medical and Technical Sciences, Chennai – 602 105, India
[b]Department of Mechanical Engineering, Saveetha Engineering College, Chennai – 602 105, India
*Corresponding author. Tel.: +91 9840106249, E-mail address: rameshphd2010@yahoo.in

Extensive research on volatile welding has focused on morphological variations at the edge [2,3], as well as the corrosion and mechanical activities of different connections [4].

But, there hasn't been much research on the topic of the explosion-bonded CP-Ti/Q345 bimetallic sheets. Due to significant variations in chemical, physical, and thermal properties, joining titanium to steel is difficult. The solubility of iron in Ti is very low, according to the Ti–Fe binary phase diagram. When the solubility of TiFe and Ti2Fe is exceeded, intermetallic phases Ti2Fe and TiFe form. These intermetallics, such as TiFe2 1500 HV and TiFe 700 HV, are relatively soft. Another critical factor that causes cracking is a thermal-stress conflict between the two components.

Even when using the solid-state joining process, the direct connection of titanium to metal is extremely hard. To achieve a reliable joint, intermediates are needed. Cu, Cr, and Ni [5] were commonly used in diffusion welding to inhibit the growth of brittle metal particles between steel and titanium. The dispersion bonding process takes more time and allows elements to be heated to high temperatures (>750 C). At high temperatures, the mechanical properties of the explosion-bonded CP-Ti/Q337 bimetallic sheets can negatively affect. [6]. The invention of high-energy beam welding techniques like laser and electron welding has recently made it probable to fuse titanium to steel [7]. Joining was made possible by inserting a 500 lm pure Cu interlayer. When compared to Titanium – Iron, and Titanium – Chromium-based stages, local production of Ti–Cu-Fe and Ti–Cu based levels had a lower impact on weld power.

Pure Copper placed between AISI316I and Ti6Al4V, on the other hand, reduced but did not eliminate the development of inelastic Titanium–Cr and Titanium–Fe-based levels. Copper was also chosen as filler metal for electron welding of titanium to steel by [9,10]. Cu reduced the remaining tensile strength in the joint and improved the metallurgical process in the igneous tub, according to the findings. [11] it was welded Ti6Al4V to 304L using an Mg interlayer and laser beam welding. Tensile intensity reached an average of 221 MPa. [12] investigated Ti6Al4V and 42CrMo laser welding. Manipulating the heating effort and resisting the development of the intermetallic reaction sheet were found to be critical for achieving a stable joint. [13] recorded using Cu filler metal to create a crack-free electron ray welded Ti6Al2Mo2V2Zr compound to 301 stainless steel connection. The compressive strength of the joint was 320 MPa. Consequently, [14] indicated that additional composite filler metals with at least two surfaces of material should be required.

Table.1 The chemical property of TI and OFC(Oxygen free copper)

Material	Elements (wt. %)									
SS304L	C	Si	Mn	P	S	Cr	Mo	Ni	N	Fe
	0.030	0.36	1.58	0.03	0.02	18.37	0.13	8.28	0.03	Bal.
	Elements (wt. %)									
Ti−6Al−4V	C		Ni		Al	V			Fe	Ti
	0.030		0.01		6.33	4.32			0.05	Bal.
	Elements (wt. %)									
OFC	Ni	P					Sn	Zn		Cu
	0.075	0.007					0.021	0.014		Bal.

Table.2 Important friction welding parameters

No.	Parameter	Joint-1	Joint-2
1	Materials	SS 304 L & copper	Copper&Ti6Al4V
2	Speed/rpm	1500	1500
3	Friction pressure/($N \cdot mm^{-2}$)	8 (20 bar)	12 (30 bar)
4	Upset pressure/($N \cdot mm^{-2}$)	14 (35 bar)	40 (100 bar)
5	Friction time/s	2	1
6	Upset time/s	8	6
7	Burn-off length/mm	7.6	11

2. Experimentalwork

2.1. Joint fabrication

Tie6Ale4V, SS301L, and oxygen-free copper were used in the experiment. Tie6Ale4V was used to make rolled round rods with a thickness of 30 mm and a size of 120 mm.

Table 3 Variable parameters forJoint-2.

Sample no.	Speed/rpm	Friction pressure/($\mathrm{N\$mm^{2}}$)	Upset pressure/($\mathrm{N\$mm^{2}}$)	Friction time (FT)/s	Upset time (UT)/s	Interlayer thickness (ILT)/mm	Remarks
1	1500	12	40	0.6	2	9	Unsuccessful joint
2	1500	12	40	0.7	3	8	Unsuccessful joint
3	1500	12	40	0.8	3.5	8	Unsuccessful joint
4	1500	12	40	0.8	4	7	Unsuccessful joint
5	1500	12	40	0.8	4.5	7	Unsuccessful joint
6	1500	12	40	0.8	4	6.15	Welded (high interlayer)
7	1500	12	40	0.9	4	5.65	Welded (high interlayer)
8	1500	12	40	1.0	5	4.85	Welded
9	1500	12	40	1.0	5	4.55	Welded
10	1500	12	40	1.1	6	1.95	Welded
11	1500	12	40	1.2	6	1.85	Welded
12	1500	12	40	1.2	6	1.16	Welded
13	1500	12	40	1.2	6.5	0.86	Welded
14	1500	12	40	1.2	7	0.72	Welded
15	1500	12	40	1.2	7	0.65	Welded

Table 4 Important process parameters.

	−1	0	1
FT (X1)	0.8	1.0	1.2
UT (X2)	5	6	7
ILT (X3)	0.65	2.65	4.65

Table 1 shows the mechanical properties and chemical composition components at room temperature of 26.50C, as determined by the ASME-E-1077-2009 standard. A rotor friction bonding machine with a fixed speed of 1600 rpm was used, as shown in Fig. 3. Table 2 and Table 3 show the normal welding parameters. As shown in Tab. 4, the specified aspects for the welding process were preferred. After deciding on the factors and levels, the experiments were carried out using the BoxeBehnken design, as shown in Table 5. In the absence of an external factorial or inverse factorial design, the BoxeBehnken design is an individual quadratic structure. The treatment combinations in this model are at the middle of the progression space's edges. These models are MOVABLE and each element needs three levels. For an experimental study, three factors and three levels are involved. The BoxeBehnken design has the highest efficiency; additionally, the number of experiments required is significantly less than for an essential composite structure. BoxeBehnken is a rotatable 2nd order architecture that was depending upon a three-level unfinished factorial model.

The samples are machined from a regular 30 mm diameter rod and then coated with abrasive cloth with a mesh size of 500e1000. This polishing produces a low surface value in hardness that was critical for friction fusing of different metals. The organized components are welded together with high pressure of 160 bars in a KUKA welding system. Figure 1 depicts the friction welding workshop. The machine's feed rate was fixed to 1.6 mm/seconds, and the experimentations were carried out according to the parameters described in Table 4.

Table 5 BoxeBehnken design.

	X1	X2	X3	FT	UT	ILT	TS
1	1	1	0	0.8	5	0.65	523.6
2	1	1	0	1.2	5	2.65	302.3
3	1	1	0	0.8	7	2.65	302.3
4	1	1	0	1.2	7	2.65	302.3
5	1	0	1	0.8	6	0.65	523.6
6	1	0	1	1.2	6	0.65	523.6
7	1	0	1	0.8	6	4.65	362.5
8	1	0	1	1.2	6	4.65	362.5
9	0	1	1	1.0	5	0.65	523.6
10	0	1	1	1.0	7	0.65	523.6
11	0	1	1	1.0	5	4.65	362.5
12	0	1	1	1.0	7	4.65	362.5
13	0	0	0	1.0	6	2.65	302.3
14	0	0	0	1.0	6	2.65	302.3
15	0	0	0	1.0	6	2.65	302.3

Plastic yielding, heat generation, and other friction-related dynamics rely heavily on process parameters. Fusing was completed in 2 stages. The first connection was initially prepared with titanium and copper rod. Because of the softness and purity of Cu combined with the elegant layer, this joint produces better performance. The copper side of the linked interface is then cut to a length of 13 mm. It is referred to the thickness of the interlayer, and the results are depicted in Figure 3. The procedure is repeated for the properties of the various sections in Tab. 4 and each example is drop checked. To determine if the bond is unchanged, drop testing is conducted instantly after the joint is developed.

Figure.1 Friction welding process set-up

Fig. 2. titanium and copper joint.

The welded example is lowered from a normal altitude of one meter to determine if the joint remains together or separates. Because of the excellent bonding achieved with the copper interlayer, the sample under analysis passed the drop test without being removed. As a result, the specimen has been taken for further examination. By observing the flashes in the samples, the main constituent was discovered to be copper. This is due to its softness and increased heat conductivity. Through machining the samples, the flashes are eliminated. Table 4 shows the thicknesses of copper. Samples are equipped as needed for the additional metallurgical and mechanical properties.

2.2. Testing the hardness:

To evaluate the appropriateness of service use, the prepared examples were exposed to hardness and tensile investigation. The samples were initially prepared for a small tensile test. This testing was performed with a 0.02 kgf 3 kgf load on an INNOVATES Vickers hardness testing system model 432D. The low load HV1 process was used in this test, which was carried out at daily intervals of 2 mm along the weld center line. HAZ causes a change in hardness along the center line.

Fig. 3. Joints with different interlayer thickness.

2.3. Flexibility test:

Static tensile investigations were conducted on samples taken from welded joints with fixed speed rotation (1600 rot/min), variable friction timing, and fixed axial pressure with or without stress concentration. With a gauge size of 45 mm and a width of 13.6 mm, the prepared specimens are tensile measured according to American standards (Fig. 4). Tensile investigation takes place at room temperature on an MTS UTM with a capacity of 1500 KN. The test examples were laden into the UTM mechanism and run through the normal testing procedure.

2.4. Micro structuretesting

Wire-cut EDM was used to prepare the samples for the microstructural analysis. The samples were prepared with different fineness’s of diamond, alumina, and magnesia, then washed and welded in hot alcohol before being etched with a reagent for 30 seconds. De-Wintortrinocular inverted metallurgical microscope with the intensification of 99 was used to examine macrostructure and microstructure using etching reagents such as Kroll's reagent for Ti alloy, pot dichromate for Cu, and Glyceregia solution for stainless steel.

Fig. 4. Fractured samples after tensile test.

3. Results

Friction welding was used to join the samples. The lattice thickness, heating time, and upset time are the main principles for joint efficiency, as shown in Fig. 5. Upset times and friction were 2.5s and 6s. After the tensile inspection, a macro analysis of the broken surface reveals significant copper diffusion on both sides. The upset times and heating for Sample 15 were 2.5s & 8s. The surface thickness in this sample was 0.70 mm, with more Cu absorbed on the stainless steel side and titanium alloy side Figure 10 depicts the hardness values of the various samples. The hardness of stainless steel ranged from 282 to 295 VHN, which was higher than the hardness of the base metal. Cu and titanium alloy have a hardness ranging from 289 VHN to 319 VHN and 78 VHN to 101 VHN, respectively. The interlayer was 0.70 mm thick and had a tensile strength of 514.5 MPa. As the interlayer width increases, the compressive strength steadily decreases. The tensile strength of the material varies between 317.5 and 519.9 MPa. With interlayer thicknesses of 0.70 to 0.90 mm, copper diffusion on all sides of the joint was fine, and compressive strength was impressive.

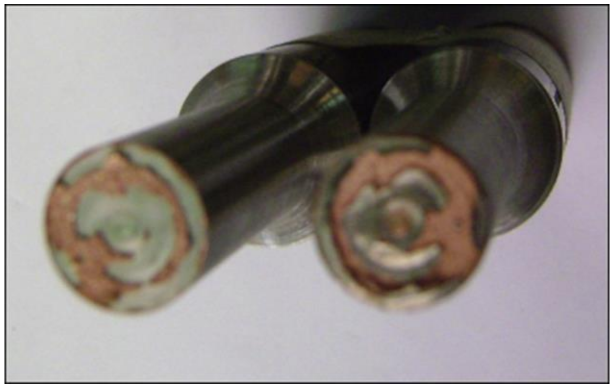

Fig. 5. Cracked face of failure sample after compressive test.

4. Discussion

4.1. Investigating the hardness:

The stainless steel hardness was improved by 12% to 23%, the Cu hardness was improved by 25%, and the titanium alloy hardness was low, according to the observed values. The increase in Cu and stainless steel side hardness was attributed to upset pressure and high-temperature rise in the weld region. Owing to intense atmospheric cooling and high upset pressure, the main metal of steel along with metal structure was altered to austenitic on the Cu side; the metal features were entirely altered with high resistance. The temperature in the lateral portion was greater than in the central region due to a higher regional velocity. It accelerated the copper, titanium, and aluminum process to improve at the edge. A higher temperature may explain the aggregation of alloying elements in the peripheral area. The phase transformed area on the SS 301L side was noticeably smaller, measuring less than 1.6 mm from the weld edge. Using an insert sheet, Fig. 6 depicts the hardness spectrum near the interface. Within 1.2 mm of the Cu interface, an incredible hardened area because of the martensite model built on the SS side.

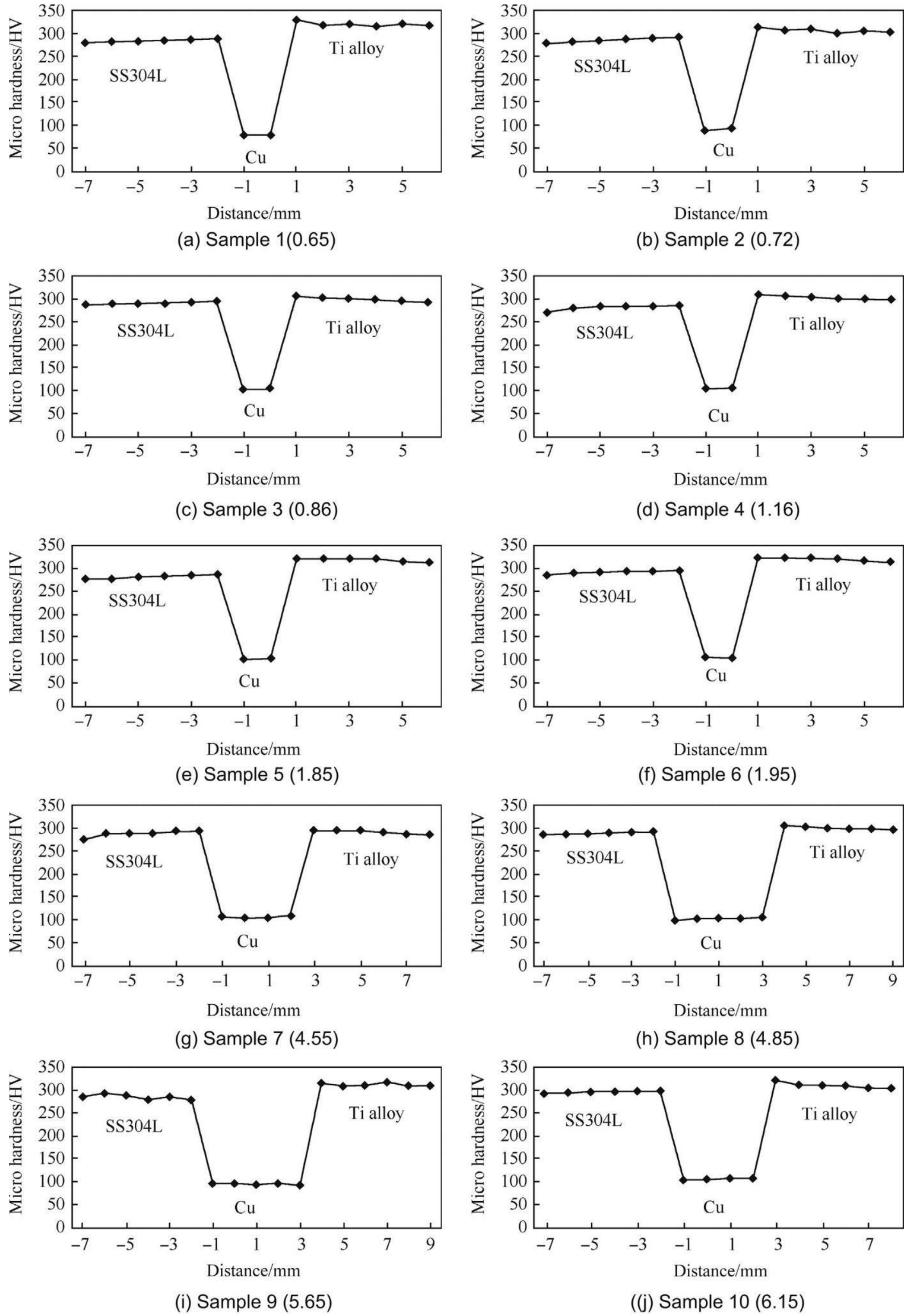

Fig. 6. Hardness of ILT samples from 1.56 to 5.95mm.

4.2. Tensile testproperties

The tensile strengths of Ti6Ale4V and X5CrNi19-12 dissimilar FW joints without interlayers were 330Mpa and 390 Mpa, respectively [8]. SS304L and pure titanium with diverse interlayer showed that the compressive strengths of Ti/Ta/SS304L, Ti/V/SS304L, Ti/Ta/Ni/SS304L, and Ti/Ni/SS304L were 415Mpa, Previous experiments on steel and titanium with no interlayer resulted in lower compressive properties of 350Mpa [8]. Cu was not used as a coating with Ti and SS314L, as shown by previous literature. The current copper interlayer research demonstrated that higher compressive strength is feasible. The overall tensile strength of 516.8 MPa was obtained during the experiments, which was similar to the power of SS304L base metal. According to the results, as the copper interlayer thickness increases, the intensity steadily decreases. Another noteworthy finding was that the connection of Cu between steel and titanium alloy was equally good due to the high resistance time of 1.3 s and the upset time of 8 s. (Fig. 9). Since copper debonding occurs at the Ti alloy side during hardness test when upsetting times and friction are low, more upset time is needed for advanced bonding. The tensile strength of TiAl and AISI 4140 steel with Cu insert layer [18] improved with subsiding layer width, with a tensile strength of about 260 MPa for a lattice thickness of 0.7mm. The maximum compressive strength was about 314 MPa or 349 MPa when the lattice width was decreased to 1.6 mm and 1.3 mm. When the titanium alloy was mixed with steel, frictional heating causes an important distortion, and the transition from titanium alpha to titanium beta occurs, along with a decrease in mechanical resistance. A quality welded joint with no defects can be enhanced by changing the resistance time while preserving axial force and fixed rotational velocity.

4.3. Microstructural investigations

An optical microscope was used to examine the prepared specimen for microstructural analysis. The main metal microstructure with Equi-axed grains of austenite can be seen in the steel matrix well away from the core. The hot extrusion of stainless steel causes several strain bands. The structure of the Ti alloy reveals the existence of an alpha step. Fig. 7(a) shows the transformation into the beta process. Due to heating and cooling, the structure of titanium alloys at the middle displays some development of alpha prime level (Fig. 7(b)).As shown in Fig. 7(c), the copper microstructure contains an alpha step in a changed beta matrix, and the interface zone between steel and Cu was analyzed as a dark distribution zone (Fig. 7(d)). The interface zone of the titanium alloy with Cu and the interface area of Titanium with copper are revealed in the (Fig. 7(e)) and (Fig. 7(f)).

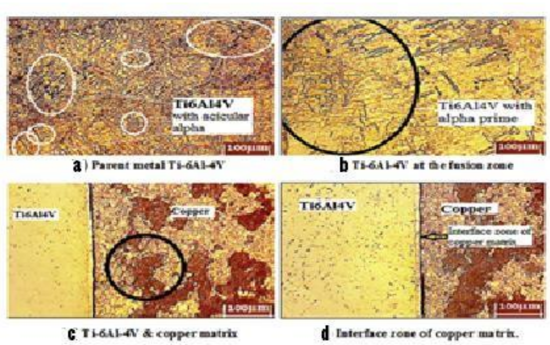

Figure 7. Microstructure of Tie6ALe4V, copper and interface region

4.4. SEM-EDSanalysis

The component distribution at the interface was determined using SEM and EDS analysis. EDS x-raysanalysis was executed on the observed findings using a 19.14 kV field affectSEM. As shown in Figure 8(a)e(c), the microstructure of the Scanning Electron Microscope of the copper and steel interface region reveals many intermetallic composites, and the result of energy dispersive x-rays are described in Tab. 6.

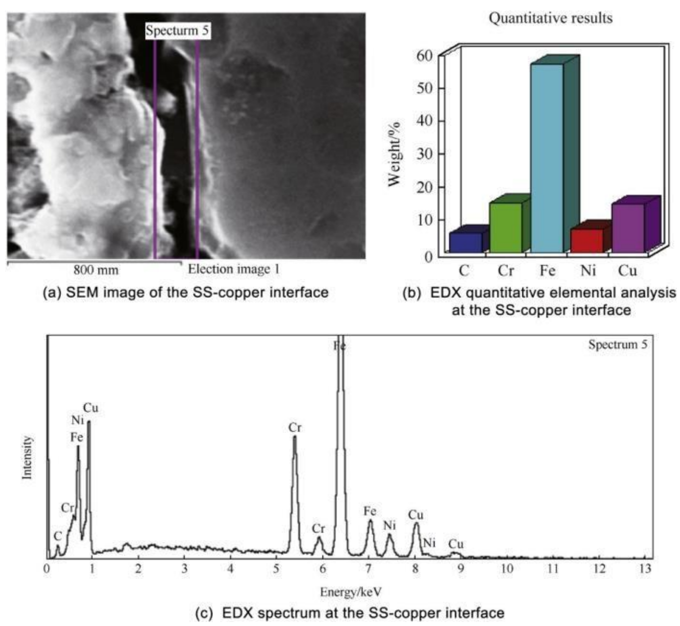

(a) SEM image of the SS-copper interface

(b) EDX quantitative elemental analysis at the SS-copper interface

(c) EDX spectrum at the SS-copper interface

Fig. 8. EDX and SEM results of Cu and steel interface.

Table 6 Components comparison of SS and base metal - Cu location.

Element	Weight% in base metal	Weight% in weld zone	Atomic/%
C K	0.030	5.75	22.29
Cr K	18.37	15.11	13.53
Fe K	71.16	57.56	47.97
Ni K	8.28	6.95	5.51
Cu K	e	14.62	10.71
Totals		100	

Copper's solubility (13.79 percent by load) was visible clearly in the area of stainless steel. The Ti alloy and copper side (Sample 3) SEM and EDX results are seenin Figure 9 and Table 7. It is also clear that the solubility of Cu in the titanium alloy was greater than that of any other element, whereas the solubility of titanium and other components such as vanadium is decreased. More copper elements dispersed on both sides of the base metal as alloying elements, according to EDS results, and there is no clear interaction between the two parent metals. In comparison to direct bonding, such an intermetallic region has high compressive and bonding strength

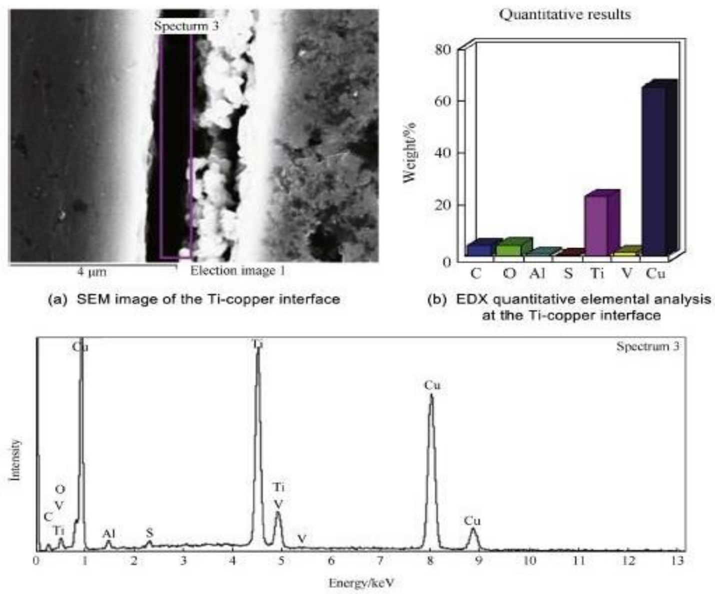

Fig. 9.EDX and SEM results of Cu and Titanium alloy

Tab. 7 Components comparison of Titanium and base metal- copper location.

Element	Weight% in base metal	Weight% in weld zone	Atomic/%
CK	0.030	4.20	15.79
OK	e	4.42	12.49
Al K	6.33	0.76	1.27
S K	0.010	0.44	0.62
Ti K	89.1	23.23	21.93
V K	4.32	1.47	1.30
Cu K	e	65.48	46.59
Total		100	

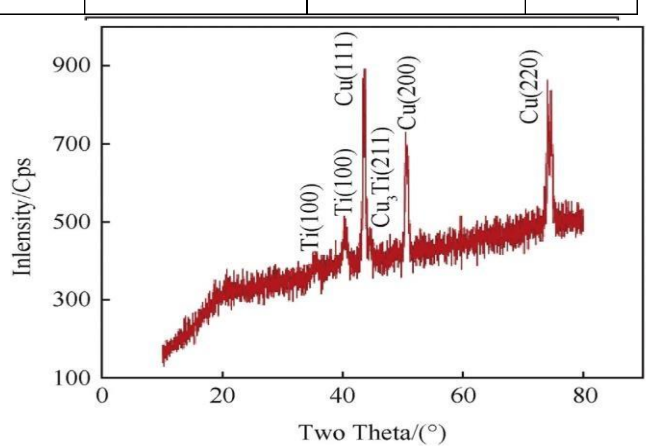

Fig. 10 Titanium and SS diffraction patterns with Cu interface.

Though the CuTi binary phase diagram shows the existence of different CueTi intermetallic phases as Cu material increases, copper's low melting point promotes a larger contact area between two sides. Welds of Ti alloys with steels are brittle due to the brittleness of the intermetallic compounds formed, such as TieCr and TieFe. XRD, EDS SEM, and tensile strength measurements were used to investigate the type and displacement of intermetallic levels in these bonds. The local aggregation of the Cu3eTi-based phase has a lower impact on the welding power, making joining possible (Fig. 10).

Conclusions

To better understand the friction welding characteristics of Tie6Ale4V and SS304L with and without copper as an interlayer, a comparative study was conducted. Based on our findings, we have come to the following conclusions.

1. Metal joints are now particularly common in the fields of defense, aerospace, automotive, biomedical, refining, and nuclear engineering. Because of their low bonding strength, some special alloys with dual phases cannot be successfully joined by friction welding. The metallurgical changes in an interfacing line on the alloy surfaces after bonding are visible.
2. When different components, such as dual-level elements were joined directly and a weak connection was detected. The inclusion of a copper interlayer in this joint was crucial in achieving a tremendous connection between steel and titanium with no cracking and protecting severe changes (martensitic) Furthermore when compared to joints formed without an interlayer, the addition of Cu as an interlayer resulted in high compressive strength of 514.7 MPa.
3. The samples with the smallest interlayer thickness obtained better results in the metallurgical and mechanical processes of the bonded samples.
4. Due to significant variations in chemical, physical, and thermal properties, joining titanium to steel is difficult. The solubility of iron in titanium is very low, according to the Titanium - Iron binary phase diagram. When the solubility of TiFe and Ti2Fe is exceeded, intermetallic phases Ti2Fe and TiFe form. These intermetallics, such as TiFe2 1500 HV and TiFe 700 HV, are relatively soft.
5. The EDS results show that more copper elements diffused as intermetallic compounds on both surfaces of the base metal, indicating that there is no clear interaction between the parent metals. The addition of a pure copper interlayer reduces the development of brittle TieFe and TieCr-based phases, which can be concluded. The local aggregation of the Cu3eTi-based phase has a lower impact on the welding power, making joining possible. As compared to direct bonding of the two steel, like an intermetallic region has increased compressive and bonding strength

References

1. Adomako, Nana Kwabena, Sanghoon Noh, Chang-Seok Oh, Sangsun Yang, and Jeoung

Han Kim. "Laser depositionadditivemanufacturingof17-4PHstainlesssteelonTi-6Al-4VusingVinterlayer." MaterialsResearch Letters 7, no. 7 (2019):259-266.
2. AlHazaa,Abdulaziz,andNilsHaneklaus."DiffusionBondingandTransientLiquidPhase(TLP)BondingofType 304 and 316 Austenitic Stainless Steel—A Review of Similar and Dissimilar Material Joints." Metals 10, no. 5 (2020):613.
3. Baharudin, B. Ariff, P. Hussain, M. Mustapha, F. Ayob, A. Ismail, F. AbRahman, P. Z. M. Khalid, D. Abdul Hamid, and M. AffendiRojan. "Tensile Properties of Diffusion Bonded Duplex Stainless Steel to Low Carbon Steel." In Advancement in Emerging Technologies and Engineering Applications, pp. 333-338. Springer, Singapore, 2020.
4. Chu, Qiaoling, Min Zhang, Jihong Li, and Cheng Yan. "Experimental and numerical investigation of microstructure and mechanical behavior of titanium/steel interfaces prepared by explosive welding." Materials Science and Engineering: A 689 (2017):323-331.

5. Cooke, Kavian O., and Anas M. Atieh. "Current trends in dissimilar diffusion bonding of titanium alloys to stainless steels, aluminium and magnesium." Journal of Manufacturing and Materials Processing 4, no. 2 (2020): 39.
6. Fang, Yongjian, Xiaosong Jiang, Defeng Mo, Degui Zhu, and ZhipingLuo. "A review on dissimilar metals' welding methods and mechanisms with interlayer." The International Journal of Advanced Manufacturing Technology 102, no. 9 (2019):2845-2863.
7. Gladkovsky, S. V., S. V. Kuteneva, and S. N. Sergeev. "Microstructure and mechanical properties of sandwich copper/steel composites produced by explosive welding." Materials Characterization 154 (2019):294-303.
8. Hosseini,SeyedRezaElmi,KaiFeng,PulinNie,KeZhang,JianHuang,YuanChen,DaShu,ZhuguoLi,BaochaoGuo, and Song Xue. "Fracture surface characterization of laser welding processed Ti alloy to stainless steel joints." Welding in the World 62, no. 5 (2018):947-960.
9. HSFL Carvalho, Gustavo, Ivan Galvão, Ricardo Mendes, Rui M Leal, and AltinoLoureiro. "Aluminum-to-Steel Cladding by Explosive Welding." Metals 10, no. 8 (2020):1062.
10. Kaya, Yakup. "Microstructural, mechanical and corrosion investigations of ship steel-aluminum bimetal composites produced by explosive welding." Metals 8, no. 7 (2018): 544.
11. Koushik, V., and D. Avinash. "Experimental investigations of friction welding using aluminium with mild steel." Int Res J EngTechnol (IRJET) 3 (2016):12.
12. Kumar Rajak, Dipen, Durgesh D. Pagar, Pradeep L. Menezes, and ArameһEyvazian. "Friction-based welding processes: friction welding and friction stir welding." Journal of Adhesion Science and Technology 34, no. 24 (2020):2613-2637.
13. Li, Jia, Junsheng Wu, Zihao Wang, Shiqi Zhang, Xiaoguang Wu, Yunhua Huang, and Xiaogang Li. "The effect of nanosizedNbC precipitates on electrochemical corrosion behavior of high-strength low-alloy steel in 3.5% NaCl solution." International Journal of Hydrogen Energy 42, no. 34 (2017):22175-22184.
14. Li, Jianxiong, Benjamin Schneiderman, S. Michelle Gilbert, AnupamVivek, Zhenzhen Yu, and Glenn Daehn. "Process characteristics and interfacial microstructure in spot impact welding of titanium to stainless steel." Journal of Manufacturing Processes 50 (2020):421-429.
15. ling Chu, Qiao, Min Zhang, Jihong Li, Qiang Jin, Qing yang Fan, Wei weiXie, HailongLuo, and Zongyue Bi. "Experimental investigation of explosion-welded CP-Ti/Q345 bimetallic sheet filled with Cu/V based flux-cored wire." Materials & Design 67 (2015):606-614.

16. Ramesh, AswinPranav, MadheswaranSubramaniyan, and PrakashEswaran. "Review on Friction Welding of Similar/DissimilarMetals."InJournalofPhysics:ConferenceSeries,vol.1362,no.1,p.012032.IOPPublishing, 2019.
17. Shinde,Gurunath,SarafarajMulani,PradipGunavant,andAbhijeetSuryawanshi."Experimentalinvestigationof friction welding on aluminium AA5083 Alloy." In Springer Proceedings of First International Conference on Energy and Environment: Global Challenges, NIT Calicut, Kerala. 2018.
18. Thirunavukarasu, Gopinath, SubrataChatterjee, and SukumarKundu. "Scope for improved properties of dissimilar joints of ferrous and non-ferrous metals." Transactions of Nonferrous Metals Society of China 27, no. 7 (2017):1517-1529.
19. Yang,Ming,JunfengXu,HonghaoMa,MingzhunLei,XiaojunNi,ZhaowuShen,BingyuanZhang,andJieTian. "Microstructure development during explosive welding of metal foil: morphologies, mechanical behaviors and mechanisms." Composites Part B: Engineering 212 (2021):108685
20. Zhang,Yan,DaQianSun,XiaoYanGu,andHongMeiLi."Microstructureandmechanicalpropertyimprovement of dissimilar metal joints for TC4 Ti alloy to 301L stainless steel." Journal of materials science 53, no. 4 (2018): 2942-2955.
21. Zhao, Hui, and Liyuan Sheng. "Microstructure and mechanical properties of the Ag/316L composite plate fabricated by explosive welding." Journal of Manufacturing Processes 64 (2021):265-275.